Asteroid Optical Navigation
Final Project Description

ASEN 5044

Fall 2023

1 Project Overview

Following the great success of NASA's OSIRIS-REx mission to asteroid Bennu,[1] an asteroid-exploration company is planning a follow-up mission to visit such a celestial body again, this time using a small satellite (SmallSat). Given its weak gravity field and the wealth of information previously gathered about Bennu's physical properties, the asteroid has been selected as the best target for the mission's technology-demonstration objectives.

A key technology proposed to fly aboard the spacecraft is the autonomous, vision-based navigation system to perform asteroid proximity operations. Current deep-space missions heavily rely on costly ground-based operations. Demonstrating autonomous capabilities would be an important stepping stone toward increasing the amount of deep-space missions and their capabilities, as well as drastically reducing operational costs.

The proposed vision-based navigation algorithm uses an onboard camera to acquire images of the asteroid surface from orbit. Images are used to detect surface landmarks, i.e., salient surface points such as boulders and craters, which can be identified from multiple orbital viewpoints. Landmarks are detected as patterns of pixels in the images. The location of one such pattern in image coordinates provides a *line-of-sight* observation, i.e., a measurement of the direction from the observing camera to the observed landmark. It is hypothesized that, by processing multiple line-of-sight measurements of surface landmarks, the autonomous-navigation system will be capable of estimating the spacecraft trajectory.

As the mission's navigation team, you are tasked with analyzing the performance of the proposed autonomous-navigation system and ultimately determine whether it is suitable for the company's mission to Bennu. You can do so using numerical simulations of (i) the spacecraft orbital motion about the asteroid, (ii) the landmark-based line-of-sight measurements, and (iii) the navigation filter itself. Figure 1 shows the simulated trajectory of the spacecraft around asteroid Bennu, plotted in the asteroid-fixed rotating frame, as well as the surface landmarks used for optical navigation. Figure 2 reports the same spacecraft trajectory plotted in the inertial (non-rotating) frame.

The information below has been provided by other mission teams to perform your navigation analysis.

1.1 State Estimation Problem

The asteroid navigation problem can be formulated as follows. Let $\mathbf{X}$ be the state vector representing the spacecraft trajectory, defined as:

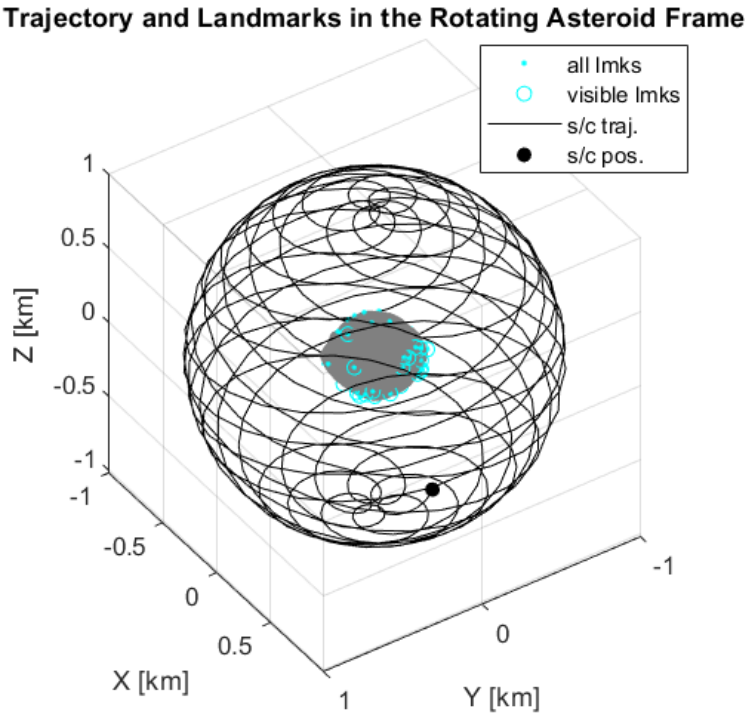

Figure 1: Spacecraft trajectory around asteroid Bennu and surface landmarks used for optical navigation, in the asteroid-fixed rotating frame. The set of landmarks visible from the last spacecraft position (circles) are highlighted.

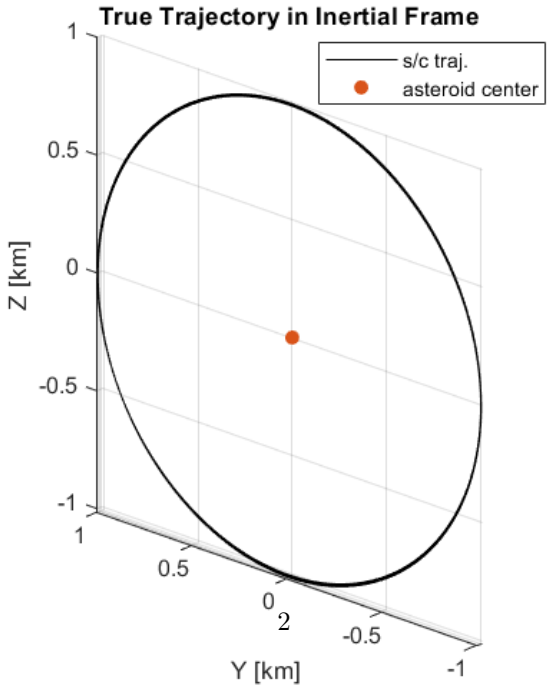

Figure 2: Spacecraft trajectory in the inertial frame.

$$\mathbf{X} = [\mathbf{r}, \dot{\mathbf{r}}]^T \tag{1}$$

$$= [x, y, z, \dot{x}, \dot{y}, \dot{z}]^T \tag{2}$$

where $\mathbf{r} = [x, y, z]^T$ and $\dot{\mathbf{r}} = [\dot{x}, \dot{y}, \dot{z}]^T$ are the spacecraft position and velocity vectors relative to the asteroid center of mass, expressed in the inertial frame shown in (Figure 2). The objective is to estimate the time evolution of the state $\mathbf{X} = \mathbf{X}(t)$ as well as the associated covariances, using line-of-sight, landmark-based observations (defined below).

2 Dynamics Model

The Flight Dynamics team suggested to study navigation performance for a so-called *terminator orbit*, similar to the one flown by the OSIRIS-REx spacecraft (Figure 2).[3] Such orbits are relatively stable despite the challenging dynamical environment of asteroids. In the vicinity of the asteroid, you can assume that there are two forces affecting the spacecraft motion: the asteroid (two-body or point-mass) gravity and the Solar Radiation Pressure (SRP).

The nonlinear spacecraft dynamics can be formulated as:

$$\ddot{\mathbf{r}} = \mathbf{f} + \tilde{\mathbf{w}} \tag{3}$$

where $\mathbf{f}$ is the nonlinear function associated with the deterministic (known) dynamics model. The nonlinear dynamics function is defined as:

$$\mathbf{f} = \mathbf{a}_{2B} + \mathbf{a}_{SRP} \tag{4}$$

where $\mathbf{a}_{2B}$ and $\mathbf{a}_{SRP}$ are the accelerations caused by the asteroid two-body gravity and by Solar Radiation Pressure (SRP), respectively. Such terms are described in Sections 2.1 and 2.2.

$\tilde{\mathbf{w}} = [\tilde{w}_x, \tilde{w}_y, \tilde{w}_z]^T$ is a process-noise term, where each component $\tilde{w}_i \sim \mathcal{N}(0, \sigma_w^2)$, $i = 1, 2, 3$, is modeled as a normally-distributed random variable with zero mean and variance σ_w^2. That is, the process noise can be considered as Additive White Gaussian Noise (AWGN), whose components are independent and identically distributed (i.i.d). Process noise is included in the dynamics model to account for stochastic, unmodeled perturbations.

2.1 Two-Body Gravity

Since the spacecraft is orbiting around the asteroid, the latter is the primary gravitational attractor. The asteroid's gravity can be approximated using the two-body (also known as Keplerian) gravity model. The spacecraft 2-body acceleration vector a_{2B} is given by:

$$\mathbf{a}_{2B} = -\frac{\mu_A}{r^3}\mathbf{r} \tag{5}$$

where μ_A is the asteroid's gravitational parameter (its mass multiplied by the gravitational constant) and $\mathbf{r}$ is the spacecraft position vector relative to the asteroid center of mass.

2.2 Solar Radiation Pressure

In the dynamical environment around low-gravity objects such as Bennu, non-gravitational forces can have a significant effect on the orbital motion. The predominant one is the Solar Radiation Pressure (SRP), caused by the photon flux emitted by the Sun and impacting the spacecraft surface. A first-order approximation of SRP effects can be obtained using the so-called *cannonball* model, whose acceleration vector $\mathbf{a}_{SRP}$ can be written as:[2]

$$\mathbf{a}_{SRP} = -\frac{\Phi_0}{|\mathbf{r}_{S/A}|^2}\left(1+\frac{4}{9}\rho\right)\frac{A}{m}\hat{\mathbf{r}}_{S/A} \tag{6}$$

where Φ_0 is the solar pressure constant, ρ is the spacecraft reflectivity coefficient, A/m is the spacecraft area-to-mass ratio, $\mathbf{r}_{S/A}$ is the position vector of the Sun relative to the asteroid center of mass, and $\hat{\mathbf{r}}_{S/A}$ is the corresponding unit vector. Observe that, in the cannonball model, the SRP effect is oriented along the direction from the Sun to the asteroid.

Importantly, observe that $\mathbf{a}_{SRP}$ does not depend on the spacecraft position, as it can be assumed that the solar flux in the region around the asteroid is uniform, i.e., its spatial gradient is negligible. This means that $\mathbf{a}_{SRP}$ can be thought of as a *known* external force, or a control input. (Hint: how does this affect the modeling and implementation of your nonlinear and linearized dynamics?)

2.3 Nominal Trajectory

When using a linearized estimation algorithm, a nominal state $\mathbf{X}_{\text{nom}}$ is required to perform linearization. In this study, you will need to propagate your own nominal trajectory, using the provided nominal initial state $\mathbf{X}_{0,\text{nom}}$. (Hint: should you include random perturbations $\tilde{\mathbf{w}}$ when propagating the nominal trajectory?)

2.4 Off-Nominal Trajectories

In reality, there is often a deviation between the true and the nominal state. Therefore, it is important to study the effect of such off-nominal deviations on estimation performance. This can be simulated numerically by (i) perturbing the initial state, with respect to the nominal, and (ii) propagating such a perturbed initial state to simulate the corresponding *true* state evolution. (When this process is performed many times and by randomly sampling the initial state deviation, we refer to it as Monte Carlo simulation.)

2.4.1 Effect of State Deviations

In the challenging dynamical environment of asteroids, state deviations can have a significant impact on trajectory evolution. Additionally, the perturbation *direction* can significantly change the evolution of the state. That is, position and velocity deviations with the same magnitude but different directions can have significantly different effects on the dynamics. As such, it is highly recommended to perturb the initial state along individual directions first, and see how each directional case affects the dynamics. It is also recommended to study the effect of position and velocity deviations individually. This will help inform and understand more advanced performance analyses.

2.4.2 A-priori Uncertainties

Other mission phases preceded proximity operations, such as approach and asteroid characterization. During these phases, the environmental uncertainties are typically reduced, and the spacecraft trajectory is refined. These estimates are then used to inform the a-priori uncertainties used for proximity operations. Thus, it is fair to assume relatively small a-priori covariance values when in close proximity with the asteroid. (Hint: for this scenario, keep the position covariances below 10 m and velocity covariances below 1 mm/s. You are encouraged to explore anisotropic covariance matrices, i.e., how different covariance magnitudes in different directions affect estimation performance. For example, what happens if you have small uncertainties on the orbit plane and large uncertainties in the direction orthogonal to the plane, or vice versa? What would happen if these uncertainties were significantly larger, for some reason? Would that inform the navigation strategy and the choice of the estimation algorithm?)

3 Measurement Model

The Spacecraft team has provided you with the specifics on the camera model to simulate line-of-sight measurements of the surface landmarks. You can use a *pinhole camera* model, where a 3D point in the scene is observed as a perfect 2D projection of that point onto the camera plane. This model assumes that error sources such as lens distortion, noise, and calibration errors, are negligible. Furthermore, you can assume that the position of the camera center (sometimes referred to as the camera focal point) coincides with the spacecraft position $\mathbf{r}$.

Thus, the observation (measurement) of a 3D landmark $\mathbf{l}$ is given by its pixel location $[u, v]^T$ within the image. These measurements can be modeled by:

$$u = f\frac{(\mathbf{l}-\mathbf{r})^T \cdot \hat{\mathbf{i}}_C}{(\mathbf{l}-\mathbf{r})^T \cdot \hat{\mathbf{k}}_C} + u_0 + \tilde{\nu}_u \tag{7}$$

$$v = f\frac{(\mathbf{l}-\mathbf{r})^T \cdot \hat{\mathbf{j}}_C}{(\mathbf{l}-\mathbf{r})^T \cdot \hat{\mathbf{k}}_C} + v_0 + \tilde{\nu}_v \tag{8}$$

where f is the camera focal length, expressed in units of pixels, $\mathbf{l}$ is the landmark position vector, and $\mathbf{r}$ is the spacecraft position vector. $\hat{\mathbf{i}}_C$, $\hat{\mathbf{j}}_C$, and $\hat{\mathbf{k}}_C$ are the unit vectors corresponding to the camera axes, such that the rotation matrix $R_{\mathcal{NC}}$, which maps a vector from the camera frame $\mathcal{C}$ to the inertial frame $\mathcal{N}$, is given by:

$$R_{\mathcal{NC}} = \left[\hat{\mathbf{i}}_C \; \hat{\mathbf{j}}_C \; \hat{\mathbf{k}}_C\right] \tag{9}$$

where $\hat{\mathbf{i}}_C$, $\hat{\mathbf{j}}_C$, and $\hat{\mathbf{k}}_C$ are the columns of the matrix $R_{\mathcal{NC}}$.

Here, it is assumed that $\hat{\mathbf{k}}_C$ is the camera boresight, i.e., the axis pointing from the camera location toward the observed scene (see Figure 3), whereas $\hat{\mathbf{i}}_C$ and $\hat{\mathbf{j}}_C$, are the horizontal and vertical axes with respect to the image, respectively. Notice that u and v are the measured pixel coordinates along $\hat{\mathbf{i}}_C$ and $\hat{\mathbf{j}}_C$, respectively.

The rotation matrix $R_{\mathcal{NC}}$ describes the orientation of the camera in space. This is typically estimated by the onboard Attitude Determination and Control System (ADCS). Thus, the numerical values of $R_{\mathcal{NC}}$ are provided to you and you simply need to plug them into the equations. Note that

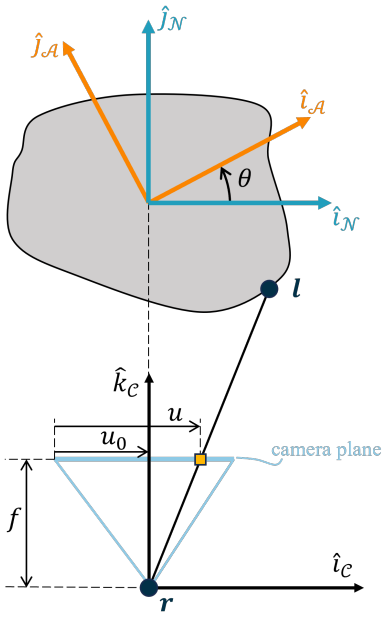

Figure 3: Graphical representation of the measurement model and observation geometry. For simplicity and ease of visualization, the schematic is presented in 2D.

the camera attitude is always *nadir-pointing*, i.e., the camera $\hat{\mathbf{k}}_C$ axis always points exactly towards the asteroid center. Also note that the camera attitude is only provided for the observation epochs.

The parameters $[u_0, v_0]^T$ represent constant offsets defining the pixel location where $\hat{\mathbf{k}}_C$ intersects the image plane. This pixel location, also known as the *principal point*, effectively represents the center of the image. (Interestingly, observe how the values of u and v do not depend on the distance $||\mathbf{l} - \mathbf{r}||$; that is, all infinite points along the line of sight $\mathbf{l} - \mathbf{r}$ yield the same $[u, v]$ values. Hence, the landmark's range cannot be directly observed with line-of-sight measurements.)

Lastly, $\tilde{\nu}_u \sim \mathcal{N}(0, \sigma_u^2)$ and $\tilde{\nu}_v \sim \mathcal{N}(0, \sigma_v^2)$ represent the measurement noise components for u and v, respectively. The two noise terms $\tilde{\nu}_u$ and $\tilde{\nu}_v$ are i.i.d. AWGN processes.

A graphical representation of the measurement model and the observation geometry is presented in Figure 3.

3.0.1 Measurement Data Format

You will be provided with a dataset of measurements to process. The dataset is in the form of a 2D matrix, where each row contains an observation and the associated metadata. In particular, each row is in the form $[t, \text{ID}, u, v]$, where t is the observation epoch in units of s, ID is the identification number of the observed landmark, whereas u and v are the actual observations, in units of pixels.

3.1 Landmark Catalog

You have been provided with a catalog of surface landmarks, selected by the Operations team using the available shape model of asteroid Bennu. Given the shape model's high resolution, you can assume that such landmarks are perfectly known, i.e., you do not need to estimate their position.

3.1.1 Asteroid-Fixed Frame

Landmarks are provided to you in the asteroid-fixed frame $\mathcal{A}$. Due to the asteroid rotational motion, the rotation between the frame $\mathcal{A}$ and the inertial frame $\mathcal{N}$ changes over time. For this analysis, you can assume that the asteroid spins about its principal axis, which coincides with the third axis, $\hat{\mathbf{k}}_A$, of frame $\mathcal{A}$. Further, you can assume that $\mathcal{A}$ and $\mathcal{N}$ coincide at the first epoch t_0, so that:

$$R_{\mathcal{N}\mathcal{A}}(t_0) = I_{3\times 3} \tag{10}$$

where $I_{3\times 3}$ is the 3×3 identity matrix.

The rotation between $\mathcal{A}$ and $\mathcal{N}$ for each subsequent time t is a pure rotation about $\hat{\mathbf{k}}_A$, such that:

$$R_{\mathcal{N}\mathcal{A}}(t) = \begin{bmatrix} \cos(\theta) & -\sin(\theta) & 0 \\ \sin(\theta) & \cos(\theta) & 0 \\ 0 & 0 & 1 \end{bmatrix} \tag{11}$$

where $\theta = \omega_A t$ is the rotation angle and ω_A is the asteroid rotation rate, which is very well known and assumed to be constant.

3.1.2 Landmarks Visibility

Not all landmarks are visible at all times. At any given time t, landmarks can be detected if both the following conditions are satisfied: landmarks shall (i) lie inside the camera field of view (FOV) and (ii) not be occluded by the asteroid itself, i.e., they shall not be on the opposite side of the surface, relative to the camera view.

Let $(u_{\max}, v_{\max})$ be the maximum image coordinates for the given camera, in units of pixels. These parameters effectively define the image resolution, which is $u_{\max} \times v_{\max}$. Then, you can check if a landmark lies inside the camera FOV based on the Boolean variable:

$$\texttt{landmark\_in\_FOV} = (0 \leq u \leq u_{\max}) \wedge (0 \leq v \leq v_{\max}) \wedge ((\mathbf{l} - \mathbf{r})^T \cdot \hat{\mathbf{k}}_C > 0) \tag{12}$$

where $\wedge$ is the logical and operator. `landmark_in_FOV` is True when the landmark is inside the camera FOV.

To check if the landmark is in front of the surface and not occluded by it, we can assume that the asteroid surface is a sphere, which is a reasonable first-order assumption for Bennu. Then, you can use the following Boolean variable:

$$\texttt{landmark\_in\_front} = \mathbf{l}^T \cdot \hat{\mathbf{k}}_C < 0 \tag{13}$$

where `landmark_in_front` is True when the landmark is in front of the surface, from the camera perspective, i.e., it is not occluded. You are invited to think about why each term in the above conditions is required to determine landmark visibility.

3.1.3 Landmarks Implementation Tip

To facilitate debugging, it is recommended to start with simplified landmark measurements. Then, you can add new components to your code step by step, aiming to maintain a working code throughout increasing levels of complexity. For instance, you could start by using a single landmark and assuming that the asteroid does not rotate with respect to the inertial frame. You could even start from creating a "fake" landmark and placing it at the center of the asteroid-fixed frame. What do the measurements look like in this case? Then, place a landmark along one of the camera axes; the measurement value along the other camera axis should be zero. Once you have "unit tested" your implementation, you can relax each of these assumptions individually.

To troubleshoot issues with landmark visibility, it may be helpful to plot both the landmarks and the spacecraft position/trajectory in the asteroid-fixed frame (as shown, for example, in Figure 1). You could plot the visible and non-visible landmarks with different markers or color codes. This way, you can visually inspect the observation geometry and determine if your visibility algorithm makes sense at a high level. For instance, if the visible landmarks are on the back side of the asteroid relative to the camera, then there is a bug in the code.

3.1.4 Landmark Data Format

You will be provided with a catalog of n_l landmark positions $\{\mathbf{l}_{\mathcal{A},1}, \ldots, \mathbf{l}_{\mathcal{A},n_l}\}$, expressed in the asteroid-fixed frame $\mathcal{A}$. The catalog is in the form of a 2D matrix, where each i-th row corresponds to the landmark whose ID is equal to i. Each row contains the x-y-z Cartesian coordinates of the corresponding landmark.

4 Simulation Parameters

The parameters required to set up the numerical simulation are reported in Table 1.

References

[1] DS Lauretta, DN DellaGiustina, CA Bennett, DR Golish, KJ Becker, SS Balram-Knutson, OS Barnouin, TL Becker, WF Bottke, WV Boynton, et al. The unexpected surface of asteroid (101955) bennu. *Nature*, 568(7750):55–60, 2019.

[2] Jay W McMahon, Daniel J Scheeres, Steven R Chesley, Andrew French, Daniel Brack, Davide Farnocchia, Yu Takahashi, Benjamin Rozitis, Pasquale Tricarico, Erwan Mazarico, et al. Dynamical evolution of simulated particles ejected from asteroid bennu. *Journal of Geophysical Research: Planets*, 125(8):e2019JE006229, 2020.

[3] DJ Scheeres, B Sutter, and AJ Rosengren. Design, dynamics and stability of the osiris-rex sun-terminator orbits. *Advances in the Astronautical Sciences*, 148:3263–3282, 2013.

Table 1: Simulation setup parameters

Parameter	Value	Units	Description
μ_A	$4.892 \cdot 10^{-9}$	$\mathrm{km}^3/\mathrm{s}^2$	Asteroid gravitational parameter (GM)
ω_A	4.296057	hours	Asteroid Rotation Period
$\mathbf{r}_S$	$[1.5 \cdot 10^8, 0, 0]^T$	km	Inertial Sun position w.r.t. the asteroid center (1 AU)
Φ_0	$1 \cdot 10^{14}$	$\mathrm{kg\,km/s}^2$	Solar pressure constant
ρ	0.4	–	Coefficient of reflectivity
A/m	$(1/62) \cdot 10^{-6}$	$\mathrm{km}^2/\mathrm{kg}$	Area-to-mass ratio
σ_w	$1 \cdot 10^{-9}$	$\mathrm{km/s}^2$	Process noise standard deviation
f	2089.7959	pixels	Camera focal length
(u_0, v_0)	(512,512)	pixels	Camera principal point coordinates
$(u_{\min}, v_{\min})$	$(0, 0)$	pixels	Min. pixel coordinates
$(u_{\max}, v_{\max})$	$(1024, 1024)$	pixels	Max. pixel coordinates
(σ_u, σ_v)	(0.25,0.25)	pixels	Measurement standard deviation
t_0	0.0	s	Initial epoch
t_f	432000.0	s	Final epoch
Δt_{int}	60.0	s	Integration time step
Δt_{obs}	600.0	s	Time step between observations
$\mathbf{r}_{0,\text{nom}}$	$[0, -1, 0]^T$	km	Nominal initial position
$\dot{\mathbf{r}}_{0,\text{nom}}$	$\left[0, 0, \sqrt{\frac{\mu_A}{\lvert\lvert\mathbf{r_0}_{,\text{nom}}\rvert\rvert}}\right]^T$	km/s	Nominal initial velocity (assuming a circular orbit)